DETECTION OF INCUMBENT RADAR IN THE 3.5 GHZ CBRS BAND

Raied Caromi, Michael Souryal, and Wen-Bin Yang

National Institute of Standards and Technology
Communications Technology Laboratory
Gaithersburg, Maryland, USA

ABSTRACT

In the 3.5 GHz Citizens Broadband Radio Service (CBRS), 100 MHz of spectrum will be shared between commercial users and federal incumbents. Dynamic use of the band relies on a network of sensors dedicated to detecting the presence of federal incumbent signals and triggering protection mechanisms when necessary. This paper uses field-measured waveforms of incumbent signals in and adjacent to the band to evaluate the performance of matched-filter detectors for these sensors. We find that the proposed detectors exceed the requirements for performance in the presence of co-channel interference from commercial long term evolution (LTE) signals, meaning that more commercial devices can use the band in the proximity of sensors. Furthermore, the detectors are robust to out-of-band emissions into this band from adjacent-band radars, which prior studies have found can be significant.

Index Terms— 3.5 GHz, CBRS, detection, environmental sensing capability, radar

1. INTRODUCTION

The CBRS in the U.S. permits commercial broadband access to the radio frequency spectrum between 3550 MHz and 3700 MHz on a shared basis with incumbents in the band [1]. Among the incumbents is the U.S. military which operates radar systems in this band, including shipborne radar off the U.S. coasts. The CBRS rules permit dynamic access to the band in the proximity of military radar provided a sensor network detects the presence of incumbent radar and triggers interference mitigation measures when necessary. The scope of this study is on the achievable detection performance of this sensor network.

In order to operate in the CBRS ecosystem, sensors must be certified to meet specific requirements. Among these requirements is the ability to detect the in-band incumbent radar signal at a minimum received power density of -89 dBm (dB relative to 1 mW)/MHz [2], within 60 seconds of onset, and with a probability of detection of 99 % or better [3].[1] With this minimum required power density, the detection is clearly

---

[1]Government requirements do not specify a maximum probability of false alarm, although this figure of merit is naturally of interest to commercial users.
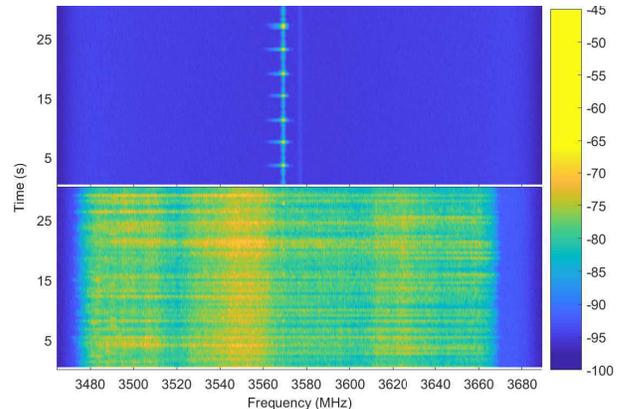

Fig. 1: Spectrograms (dBm) of measured in-band incumbent radar [5].

not thermal-noise-limited, as the detection threshold is 25 dB above the thermal noise floor. The challenge for detection is presented, rather, by co-channel interference.

There are two primary sources of co-channel interference at the sensor's receiver. First, by design, the band is shared with commercial systems. Therefore, sensors must be able to detect the incumbent signal in channels occupied by commercial systems. These systems are expected to be fourth-generation LTE systems, at least initially. However, the emissions of commercial systems operating in the band can, in principle, be controlled by treating the sensors as protected entities in the CBRS system.

The second, more challenging, source of interference is the out-of-band emissions of systems operating in adjacent bands. These systems are also military radars, operate at frequencies below the CBRS band, and have been observed to generate significant emissions into the CBRS band [4, 5]. Fig. 1 shows the first 30 s of two spectrograms of the measured in-band SPN-43 radar present at 3570 MHz, one with and one without adjacent-band emissions.

This paper is a study of the performance of a class of detectors, namely matched-filter detectors, matched to the current in-band radar system and under realistic conditions of co-channel interference. This study leverages actual waveform recordings of both the in-band radar and the out-of-band emissions of adjacent-band radars collected in field measurements conducted at two U.S. coastal locations [4, 5]. We

present the achievable tradeoff between detection and false-alarm rates under different interference conditions for two variants of the matched filter (MF) detector, coherent and non-coherent. While this study is limited to detection of the current in-band radar, SPN-43, a similar analysis can be performed for future radars deployed in this band.

Detection by CBRS sensors differs from traditional radar detection primarily because the sensor aims to identify the presence of a radar signal rather than detecting and tracking a target. Additionally, unlike a typical radar receiver that has full access to the radar waveform, the sensor has only partial knowledge of radar waveform parameters. However, elements of classical radar detection can still be utilized. In particular, we use coherent and non-coherent MF detectors [6]. A comparable problem to the detection of incumbent radar in the $3.5\,\mathrm{GHz}$ band is the protection of radars in the $5\,\mathrm{GHz}$ band, namely, dynamic frequency selection (DFS) in wireless access systems. DFS systems must avoid, or vacate, a channel identified as being occupied by the radar. However, the detection requirement is more relaxed than in CBRS; for instance, the detection threshold for the lower-power wireless devices is $-62\,\mathrm{dBm}/18\,\mathrm{MHz}$ [7]. Furthermore, it is not clear that adjacent-band emissions are as much an issue as in CBRS.

2. SIGNAL MODEL

The $3.5\,\mathrm{GHz}$ CBRS band provides access to a total of $150\,\mathrm{MHz}$ bandwidth divided into 10 MHz channels. A sensor is required to detect the presence of in-band radar in any channel of the lower $100\,\mathrm{MHz}$ of the band, and multiple radar signals may be present in different channels. A capable sensor can simultaneously or sequentially acquire the signal from all channels in order to identify the possible presence of incumbent radar signals. Alternatively, a sensor may employ multiple detectors in parallel, for instance, one per channel.

Therefore, we simplify the signal model by assuming a single channel which may or may not be occupied by the incumbent in-band radar signal. In addition, we consider three types of noise: gaussian thermal noise, co-channel commercial LTE emissions, or adjacent-band radar emissions. The simplified model of the received baseband signal, then, is

$$x[n] = s[n] + v[n],$$

where s is the in-band radar signal whose presence we are trying to detect, and v is either complex white gaussian noise (CWGN), an LTE signal, or emissions from an adjacent-band radar.

3. INCUMBENT RADAR DETECTION

The statistical hypothesis testing for a single radar signal detection is

$$\begin{cases} H_0 : x[n] = v[n], \\ H_1 : x[n] = s[n] + v[n]. \end{cases}$$

If no interference is present, and $s[n]$ is known, the problem becomes the classical detection of a known complex deterministic signal in CWGN [8]. The optimal detector for this case is a MF (or equivalently, a replica correlator). A true MF detector requires perfect knowledge of the signal. We assume the pulse repetition interval and pulse duration are approximately known based on prior observation [4, 5]. Other parameters of the radar signal are simply unknown. For instance, neither the frequency nor the phase information is known a priori. Obviously, disregarding the phase information for the coherent detector will degrade the performance. However, the issue of not knowing the center frequency of the radar signal can be resolved by implementing a bank of MFs over the entire baseband. Prior observations [4, 5, 9] indicate that these radars typically operate on a 10 MHz grid.

Let $\hat{s}(t)$ be a template for the incumbent radar signal, defined as

$$\hat{s}(t) = \exp(j2\pi f_0 t)p(t),$$

where f_0 is the center frequency of the template in the baseband, and $p(t)$ is a train of rectangular pulses. If the number of pulses in $p(t)$ is equal to L, then

$$p(t) = \begin{cases} 1, & t \in [\ell T_{pr}, \ell T_{pr} + T_{pw}], \ell = 0, 1, \ldots L-1 \\ 0, & \text{otherwise}, \end{cases}$$

where T_{pw} is the pulse width, and T_{pr} is the pulse repetition interval in seconds. Let $\hat{s}[n]$ be the sampled version of $\hat{s}(t)$. The impulse response of the MF is $h[n] = \hat{s}^*[-n]$. The output of the MF is given by the convolution $x[n] \circledast h[n]$. Alternatively, the same result can be obtained from the deterministic cross-correlation given by

$$r_{xs}[m] = \sum_{n=-\infty}^{\infty} x[n]\hat{s}^*[n+m], -\infty < m < \infty.$$

In practice we compute $r_{xs}[m]$ for the lag values $m = 0, \pm1, \pm2, \ldots, \pm(N-1)$, where N is the number of samples of $x[n]$. Let test statistic of the detector $\mathcal{T}\{r_{xs}[m]\}$ be a function of the output of the cross-correlator. The decision rule is given by

$$\mathcal{T}\{r_{xs}[m]\} \underset{H_0}{\overset{H_1}{\gtrless}} \gamma,$$

where γ is the detection threshold for the MF. The probability of detection and the probability of false alarm are given by

$$P_D = P_r\left(\mathcal{T}\{r_{xs}[m]\} > \gamma \mid H_1\right),$$
$$P_{FA} = P_r\left(\mathcal{T}\{r_{xs}[m]\} > \gamma \mid H_0\right),$$

respectively. It is straightforward to calculate closed forms of these probabilities for a known signal in white gaussian noise (WGN) [6, 8]. However, we use empirical methods to estimate these probabilities since we do not have full knowledge of the signal, and the interference is not WGN.

4. PERFORMANCE ANALYSIS

We test two types of MF detectors. The first type is coherent MF. The input to the filter for this type is the complex

signal, and thus we label it complex correlator (CC). For the second type, non-coherent MF, the input to the MF is the signal stripped of its phase, i.e., $|x[n]|$. We label this filter as magnitude correlator (MC). The test statistic for CC is the maximum value of $|r_{xs}[m]|$ over all values of m. The MC, on the other hand, benefits from a different test statistic. Specifically, $\mathcal{T}\{r_{xs}[m]\}$ is the sum of the magnitudes of L pulses from the output of the correlator. The sum is computed by aligning the pulses at the output of the filter.

Field-measured signals of shipborne radar are used in the simulation for both in-band and adjacent-band radar signals. These waveforms were originally $60\,\text{s}$ in duration, sampled at $225\,\text{MHz}$. We first decimate these waveform files to a $25\,\text{MHz}$ sampling rate. For the in-band radar waveforms, we shift the signals so that they are centered at zero baseband frequency. A large set of waveform files with strong in-band and adjacent-band radar signals is selected for simulations. For each in-band radar waveform file, (8 to 15) segments are extracted for simulation. Each segment is $20\,\text{ms}$ long, which is approximately the time it takes for the main beam of the radar antenna to illuminate the detector as the radar antenna rotates in the azimuth plane. The radar segments, in addition to the interference signals, are further filtered and downsampled to $2\,\text{MHz}$ in order to reduce the computational time of the MF. A total of $16\,000$ different radar segments with SNR higher than $30\,\text{dB}$ of the in-band radar signals are used for performance evaluation. Each evaluation consists of simulating both radar present and radar absent cases.

We choose a MF template of $10\,\text{ms}$. Since the signal is $20\,\text{ms}$ in duration, the template is padded with zeros for the difference in time length. Based on the analysis provided in [4, 5], we set $T_{pr} = 1\,\text{ms}$, and $T_{pw} = 1\,\text{µs}$, i.e., $L = 10$. We define SNR as the peak power of the radar signal to the average noise power in $1\,\text{MHz}$. However, since the $20\,\text{ms}$ segments includes 20 pulses of the radar signal, we use the average of the peak power of these pulses for the SNR and peak power settings. Although the original waveform captures include noise, its effect is ignored since the waveforms have high SNR values. However, the waveform captures include channel fading effect. The in-band radar signals are added to either WGN, LTE, or adjacent-band interference to generate realistic scenarios similar to what an actual sensor will observe. Radar signal power levels are adjusted to the desired SNR or desired radar peak power values.

4.1. Ideal signal detection in WGN

We first evaluate the detection performance when an actual radar signal extracted from field measurements is used as the template. The same template is then used as a signal after corrupting it with WGN and delaying it with a random time delay at each iteration of the simulation. Fig. 2 shows the achievable receiver operating characteristic (ROC) curves for this case. As expected, CC performs better than MC for this
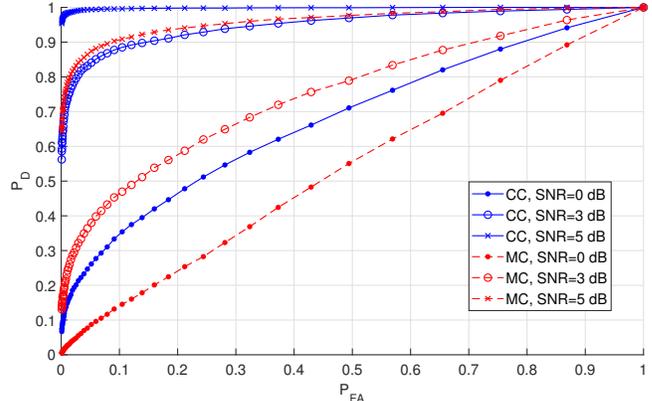

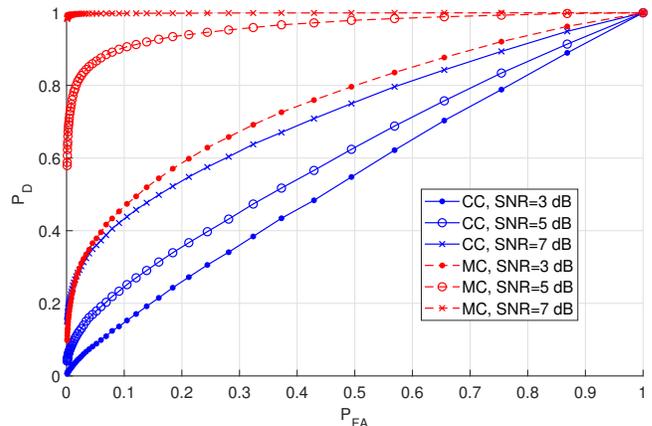**Fig. 2**: Measured signal as template; signal with added WGN.

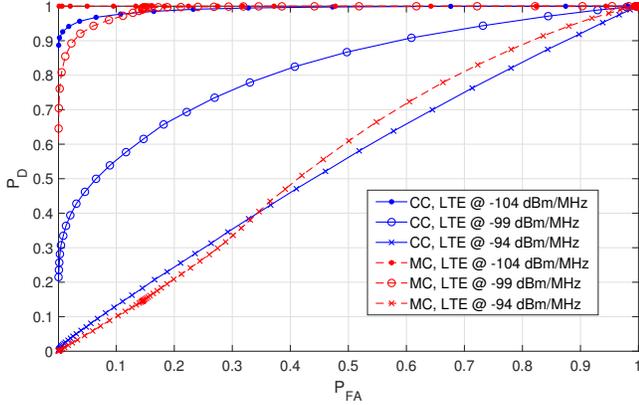**Fig. 3**: Synthetic template; signal with added WGN.

case since the template contains the original phase information and the coherent detector performs to its fullest. In practice, a sensor will not have a priori access to the actual signal for use as the template. Therefore, this example demonstrates the best-case detection performance of a sensor.

4.2. Signal detection in WGN with synthetic template

For a realistic detection case, we use a synthetically generated pulse template. We use all $16\,000$ radar signal segments in the detection performance evaluation. The signals were corrupted with noise with a fixed power level, and the radar signal amplitudes were adjusted for specific SNR values. The threshold values were estimated from the cumulative distribution function (CDF) of the noise for a given set of P_{FA} values. Fig. 3 shows the ROC curves for both CC and MC detectors. Clearly, MC performs better than CC due to unmatched phase between CC template and the radar signal. In addition, the difference between the performance of the perfectly matched filter, i.e., the CC detector in Fig. 2, and the MC detector in Fig. 3 is approximately $2\,\text{dB}$ in SNR, which represents the loss from using the synthetic template instead of a perfectly matched detector.

Table 1: LTE TDD configurations

TDD uplink/downlink configuration	0	1	2	3	4	5	6
Modulation and coding scheme index uplink/downlink[2]	6/6	12/12	24/12	14/16	4/12	5/16	24/6
Number of physical resource block uplink/downlink[3]	50/15	50/50	25/50	50/50	15/50	6/50	50/6
Downlink to uplink power ratio dB	0	1	2	3	0	1	2

Fig. 4: Synthetic template; signal with LTE interference.

4.3. Detection in LTE interference

We subject the detectors to a single interfering LTE time division duplex (TDD) signal, representing a nearby dominant interferer. The LTE signals are set to be co-channel with the in-band radar signals. LTE TDD waveforms are generated with commercial software. At each iteration of the simulation, the LTE frame structure is randomly selected from the 7 TDD configurations in Table 1. Each configuration defines which subframes are utilized for downlink and for uplink. For each TDD configuration, we configure the LTE waveforms as shown in the table. The peak power of the radar signals is set at the required detection threshold of $-89\,\mathrm{dBm/MHz}$. Fig. 4 shows the ROC curves for multiple values of received LTE average power per $1\,\mathrm{MHz}$.

Note that sensors are required to tolerate only $-109\,\mathrm{dBm/MHz}$ of aggregate commercial emissions [2]. These results indicate, therefore, that the MC detector can tolerate $10\,\mathrm{dB}$ more commercial interference than required.

4.4. Detection in adjacent-band interference

For this case, measured adjacent-band signals are added to the in-band radar signals. The SNR for the in-band radar is set to $19\,\mathrm{dB}$. The generated waveforms are similar to the in-band radar with adjacent-band emissions shown in Fig. 1, but the power levels of the in-band and adjacent-band signals are set separately. We first extract strong adjacent-band bursts from the field-measured waveforms. We divide these emissions into three sets based on the peak interference to noise ratio (INR). The $>30\,\mathrm{dB}$ set has a median INR of $34\,\mathrm{dB}$ and a maximum INR of $72\,\mathrm{dB}$.

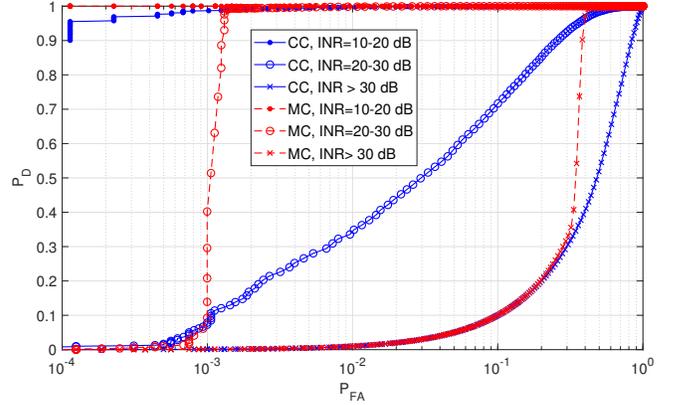[2]Table 7.1.7.1-1 [10]
[3]Table 7.1.7.2.1-1 [10]

Fig. 5: Synthetic template; signal with measured adjacent-band radar emissions.

Fig. 5 shows ROC curves for multiple interference levels. We observe that, even with adjacent-band emissions at peak INR levels of $20\,\mathrm{dB}$ to $30\,\mathrm{dB}$, the MC detector can achieve near perfect detection with a false alarm probability of only 10^{-3}. However, at higher interference levels, the false alarm rate increases to $40\,\%$.

5. CONCLUSION

We presented an analysis of federal incumbent detectors for the $3.5\,\mathrm{GHz}$ shared-spectrum CBRS band using field-measured signals of the in-band incumbent radar as well as of adjacent-band emissions into this band, which prior studies have shown to be significant. While coherent detection is shown to be superior with known signals in WGN as expected, a practical magnitude-correlator detector outperforms the coherent detector in the absence of phase information of the in-band radar. The magnitude detector performs well at a peak SNR of $5\,\mathrm{dB}$ in gaussian noise, but with interference from commercial CBRS (LTE) devices, a peak SIR of $10\,\mathrm{dB}$ is needed, suggesting that a single, dominant LTE signal is not well modeled by gaussian noise. Nevertheless, the detector's performance exceeds current requirements, meaning that more commercial devices can use the band in the proximity of sensors. Finally, the MC detector is quite robust to adjacent-band emissions having peak INR levels as high as $20\,\mathrm{dB}$ to $30\,\mathrm{dB}$.

In ongoing work, we are examining the effectiveness of machine-learning algorithms for detection of the incumbent radar in the presence of commercial LTE and adjacent-band emissions. While this study focused on detection of the current radar in the band, future work may address the detection of future radars entering this band.

6. REFERENCES

[1] "Citizens broadband radio service," 2 C.F.R. § 96, 2016.

[2] Frank H. Sanders, John E. Carroll, Geoffrey A. Sanders, Robert L. Sole, Jeffery S. Devereux, and Edward F. Drocella, "Procedures for laboratory testing of environmental sensing capability sensor devices," Technical Memorandum TM 18-527, National Telecommunications and Information Administration, Nov. 2017.

[3] "Requirements for commercial operation in the U.S. 3550–3700 MHz citizens broadband radio service band," Wireless Innovation Forum Document WINNF-TS-0112, Version V1.5.0, May 2018.

[4] Paul D. Hale, Jeffrey A. Jargon, Peter J. Jeavons, Michael R. Souryal, Adam J. Wunderlich, and Mark Lofquist, "3.5 GHz radar waveform capture at Point Loma: Final test report," Technical Note 1954, National Institute of Standards and Technology, May 2017.

[5] Paul D. Hale, Jeffrey A. Jargon, Peter J. Jeavons, Michael R. Souryal, Adam J. Wunderlich, and Mark Lofquist, "3.5 GHz radar waveform capture at Fort Story: Final test report," Technical Note 1967, National Institute of Standards and Technology, Aug. 2017.

[6] Mark A. Richards, *Fundamentals of Radar Signal Processing, Second Edition*, McGraw-Hill Education, 2014.

[7] "Dynamic frequency selection in wireless access systems including radio local area networks for the purpose of protecting the radiodetermination service in the 5 GHz band," Recommendation ITU-R M.1652-1, 2011.

[8] Steven M. Kay, *Fundamentals of Statistical Signal Processing: Detection theory*, Prentice Hall Signal Processing Series. Prentice-Hall PTR, 1998.

[9] Michael G. Cotton and Roger A. Dalke, "Spectrum occupancy measurements of the 3550-3650 megahertz maritime radar band near San Diego, California," Technical Report TR 14-500, National Telecommunications and Information Administration, Jan. 2014.

[10] "LTE-evolved universal terrestrial radio access (E-UTRA) physical layer procedures," 3GPP Std. TS 36.213, V10.3.0 Release 10, 2011.